Vol. 526: 41–53, 2015
doi: 10.3354/meps11249

MARINE ECOLOGY PROGRESS SERIES
Mar Ecol Prog Ser

Published April 22

Shifts in sponge-microbe mutualisms across an experimental irradiance gradient

Christopher J. Freeman[1,2,*], David M. Baker[3], Cole G. Easson[2], Robert W. Thacker[2]

[1]Smithsonian Marine Station, Fort Pierce, Florida 34949, USA
[2]Department of Biology, University of Alabama at Birmingham, Birmingham, Alabama 35294, USA
[3]The Swire Institute of Marine Science, School of Biological Sciences & Department of Earth Science, University of Hong Kong, Hong Kong, PR China

ABSTRACT: To investigate how the interactions between the closely related sponge species *Aplysina cauliformis* and *Aplysina fulva* and their symbiotic microbial communities vary under changing environmental conditions, we conducted a manipulative shading experiment with treatments spanning a gradient of 6 irradiances. In *A. cauliformis*, there was a tight coupling of symbiont and host metabolism across treatments, and changes in growth rate were correlated more with shifts in symbiont $\delta^{13}C$ and $\delta^{15}N$ values than with shade treatment. In contrast, symbiont and host C metabolism were weakly coupled in *A. fulva*, and the growth of this species was not correlated with shifts in symbiont $\delta^{13}C$ and $\delta^{15}N$ values. In addition, although photosymbiont metabolism was an important driver of shifts in holobiont C and N metabolism of both host species, host and photosymbiont C metabolism were only correlated in *A. cauliformis*. Thus, although both species host stable, abundant, and similar photosymbiont communities, each host forms a unique mutualism with its symbionts. These 2 host species may be on different evolutionary trajectories, potentially allowing each to exploit novel niche space in coral reef ecosystems. This study provides data in support of the hypothesis that these symbioses represent a dynamic balance of costs and benefits and provides evidence that, because these costs and benefits are highly species-specific, not all species will respond similarly to environmental fluctuations.

KEY WORDS: Stable isotopes · Metabolism · Mutualism · Porifera · Symbiosis

INTRODUCTION

By forming complex interactions with microbial symbionts, many eukaryotic hosts gain access to a vast array of goods and services that would not be available without a symbiont partner (Boucher et al. 1982). Benefits such as the products of autotrophic and chemosynthetic metabolism allow host species to survive and compete for space in systems that, in many cases, would be otherwise inhospitable (Steinert et al. 2000, Nyholm & McFall-Ngai 2004, Dattagupta et al. 2009). In return, many of these symbionts are provided a protected habitat and a supply of nutrients from the host (Herre et al. 1999, Vrijenhoek 2010). Within oligotrophic reef ecosystems, these mutually beneficial interactions are exemplified by taxa like corals and sponges that supplement their heterotrophic feeding with the autotrophic metabolism of abundant dinoflagellate or microbial symbiont communities (Muscatine et al. 1989, Stanley 2006, Thacker & Freeman 2012). In such systems, host survival and performance may be contingent on these supplementary nutrient inputs (Barneah et al. 2004, Venn et al. 2008, Zilber-Rosenberg & Rosenberg 2008, Thacker & Freeman 2012).

Because these interactions include both benefits and costs, an association can only be considered mutually beneficial when these benefits exceed the costs of maintaining a symbiosis (Bronstein 2001, Wooldridge 2010). Indeed, natural selection favoring symbioses with a low cost to benefit ratio (CBR) to each member might lead to the evolution of stable

*Corresponding author: freemanc@si.edu

symbioses between specific host and symbiont genotypes (Johnson & Graham 2013, Freeman et al. 2013). Factors such as changing environmental conditions, nutrient cycling and resource competition between different symbiont genotypes within a host and the colonization of the host by novel symbiont taxa might destabilize these symbioses and shift the CBR of the association (Thacker & Freeman 2012). Ultimately, as costs exceed benefits, a mutualistic interaction may become parasitic (Boucher et al. 1982, Bronstein 2001, Thacker & Freeman 2012). Symbiont theory thus predicts that these symbioses exist along a continuum from mutualism to parasitism (Herre et al. 1999).

A balance between the costs and benefits of symbiotic interactions is well described in some terrestrial and marine systems. For example, plant hosts and mycorrhizal fungal symbionts exchange the commodities of fixed carbon and soil-derived nitrogen and phosphorus, respectively (Cowden & Peterson 2009). To maintain an optimal CBR, the plant supplies enough carbon to the fungus to obtain adequate nutrients while simultaneously reserving sufficient fixed carbon for its own growth requirements (Johnson & Graham 2013). As irradiance is reduced or soil nutrient concentrations are increased, however, the cost to the host of maintaining this interaction can increase beyond its benefit (Johnson & Graham 2013). Likewise, although reef-building corals obtain a predominant portion of their carbon from intracellular dinoflagellate symbionts, changes in environmental conditions can cause shifts in the CBR that ultimately lead to the expulsion of symbionts from the coral host (Wooldridge 2013). Although reports of symbioses in other coral reef organisms have increased in recent years, we still know surprisingly little about how these interactions are impacted by environmental change.

Many marine sponges host a biodiversity of microbial symbionts that is unparalleled in other invertebrates, forming associations with members of almost all evolutionary lineages of bacteria and archaea (Webster et al. 2010, Schmitt et al. 2012, Thacker & Freeman 2012). These communities are highly species-specific, suggesting that sponge hosts exert a strong influence on their symbiont community (Taylor et al. 2007, Schmitt et al. 2012, Easson & Thacker 2014). In addition, although some species (termed High Microbial Abundance [HMA]) host abundant symbiont communities, other sympatric species host only sparse symbiont communities (termed Low Microbial Abundance [LMA]) (Taylor et al. 2007, Weisz et al. 2007). Surprisingly, while LMA species appear to meet their energy demands via heterotrophic feeding on local sources of organic matter, the relative importance of heterotrophic feeding and symbiont-derived nutrition is highly variable across HMA species (Wilkinson 1983, Weisz et al. 2007, Freeman & Thacker 2011, Freeman et al. 2013).

For instance, although the closely related host species *Aplysina cauliformis* and *Aplysina fulva* both support abundant, genetically similar, and equally productive photosymbiont communities (Erwin & Thacker 2007, 2008a, Thacker & Freeman 2012), *A. cauliformis* assimilates approximately 70% of its C from its symbiont community, whereas *A. fulva* assimilates only 45% of its C from this source (Freeman & Thacker 2011). Furthermore, host metabolism appears to be tightly coupled to that of the symbiont community in *A. cauliformis*, even under experimental shading. Under these same conditions, however, host and symbiont communities were increasingly decoupled in *A. fulva* (Freeman & Thacker 2011). These data, along with a significant reduction in the growth rate of *A. fulva* but not *A. cauliformis* under shade conditions, provide compelling evidence that these interactions, and their functional responses to environmental change, are fundamentally distinct (Freeman & Thacker 2011, Thacker & Freeman 2012).

To further investigate these interactions and how they change with irradiance, we held individuals of *A. cauliformis* and *A. fulva* under shade canopies representing a gradient of 6 levels of light availability. We assessed whether host benefit (host growth rate) was driven by shifts in photosymbiont abundance (chlorophyll *a* concentration) or symbiont and host metabolism ($\delta^{13}C$ and $\delta^{15}N$ values of isolated microbial and sponge cell fractions). We also evaluated whether host and symbiont C and N metabolisms were coupled by comparing $\delta^{13}C$ and $\delta^{15}N$ values of the sponge cell fraction to those of the corresponding microbial fraction. In addition, at the end of the experiment, we incubated individuals of both species from the highest (control), intermediate, and lowest irradiance treatments in seawater containing inorganic compounds enriched in ^{13}C and ^{15}N to determine how the productivity of the sponge–microbe association (holobiont) and the efficiency of photosymbiont and host C and N metabolism were impacted by these incubations (Freeman et al. 2013). Finally, because the presence or absence of particular clades of the sponge-specific cyanobacterium *Synechococcus spongiarum* might drive trends in holobiont productivity and C and N cycling (Thacker & Freeman 2012), we used temperature gradient gel

electrophoresis (TGGE) to profile the clades of *S. spongiarum* present in individuals of both host species from each treatment.

MATERIALS AND METHODS

Study organisms

Aplysina cauliformis and *A. fulva* were collected from STRI Point (9° 20′ 55.24″ N, 82° 15′ 45.95″ W), a shallow (3 to 5 m) reef adjacent to the Smithsonian Tropical Research Institute (STRI) in Bocas del Toro, Panama. Ten large (~80 cm long) individuals of each species were transported to aquaria at STRI, where each individual was divided into 7 (~10 cm long) pieces. A portion of the initial piece was sectioned into ~1 cm^3 slices and placed in 95% EtOH for future TGGE analyses. The remainder of this piece was wrapped in aluminum foil and frozen for initial measurements of stable isotope ratios ($\delta^{13}C$ and $\delta^{15}N$) and chlorophyll *a* (chl *a*), while the other 6 pieces were carefully blotted dry and weighed to the nearest 0.01 g to obtain an initial wet weight. After weighing, pieces were returned to flowing seawater tanks, where they were allowed to acclimate overnight.

Shading experiment

Our canopy design was adapted from that of Freeman & Thacker (2011), modified to provide a gradient of irradiance across treatments. In place of only clear (control) and dark (shade) canopies, we used clear canopies covered by varying layers of fiberglass window screening. Five canopies lacking window screening, herein referred to as control canopies, and 5 canopies of each shade treatment (covered by 1 to 5 layers of window screening, herein referred to as treatments S1 [1 layer] to S5 [5 layers]) were constructed as described by Freeman & Thacker (2011); window screening layers were attached to canopies using plastic cable ties. Control canopies were transparent to visible light, providing approximately 75% of ambient light, while canopies in treatment S5 provided <5% of ambient light (as in Freeman & Thacker 2011). Intermediate treatments S1, S2, S3, and S4 allowed 30, 25, 15, and 8% of ambient light, respectively, as monitored by HOBO (Onset) data loggers deployed underneath the canopies during the course of the experiment and by measuring photosynthetically active radiation (PAR) under each canopy using a Licor underwater spherical quantum sensor (Ll-193) coupled to a Licor Li-250A light meter.

One piece each from 2 individuals of *A. fulva* and *A. cauliformis* was deployed under each canopy, yielding a total of 30 canopies (5 each of control and treatments S1 through S5), each holding 2 replicates of each species. Sponges were attached to canopy bases using cable ties, and canopies were deployed in the field on a 4 m deep patch reef at STRI point, approximately 10 m horizontally from where sponges were initially collected. Canopies were monitored and cleaned twice each week. Samples of particulate organic matter (POM), a potential source of organic matter to sponges feeding heterotrophically, were collected weekly and processed as described by Freeman & Thacker (2011).

After 73 d, canopies were collected, and final blotted wet weights were measured for each sponge individual. Growth rates were calculated as relative change [(final mass − initial mass) (initial mass)$^{-1}$]. Sponges were excluded from this analysis if they displayed predation scars or tissue necrosis. At least 4 replicates of *A. cauliformis* and *A. fulva* from each treatment were sectioned into 1 cm^3 subsamples and placed in 95% EtOH for TGGE analyses as above. The remainder of each piece was wrapped in aluminum foil and frozen. The remaining replicates of both species from treatments S1, S3 and S4 that had been weighed but not sectioned were wrapped in aluminum foil and frozen for chlorophyll *a* (chl *a*) and isotope analyses. Samples that had been weighed, but not sectioned, from control, S2, and S5 canopies were returned to flowing seawater tables and allowed to acclimate overnight prior to bottle incubations using tracers enriched in ^{13}C and ^{15}N.

$\delta^{13}C$ and $\delta^{15}N$ tracer experiment

To determine whether shading experiments impacted symbiont productivity and the efficiency of nutrient assimilation and transfer, we used methods adapted from Freeman et al. (2013). In short, 98 atom% ^{13}C $NaH^{13}CO_3$ and 98 atom% ^{15}N $Na^{15}NO_3$ were added to filtered (0.70 µm GF/F, Whatman) seawater to final concentrations of 1.18 and 0.117 mM, respectively. This enriched seawater was then partitioned among 24 Nalgene HDPE translucent bottles (500 ml volume, ~50% of ambient light transmitted). Unlike in Freeman et al. (2013), the present study did not include dark bottles in these incubations because doing so would have required us to partition replicates from the shading experiment, some of which

had lost considerable mass during the experiment. Initial dissolved oxygen (DO, mg l^{-1}) concentrations were measured using a WQ-DO (NexSens Technology) dissolved oxygen sensor. Bottles were incubated under natural sunlight in a flowing seawater table for 6 h. Irradiance and temperature were recorded every 2 min during these incubations using HOBO loggers attached to the exterior of the incubation tank and within light bottles containing water but no sponges. After 6 h, final DO (mg l^{-1}) concentrations were measured; sponges were removed from the bottles, blotted dry, weighed, wrapped in aluminum foil, and frozen for chl *a* and isotope analyses.

NPP and chlorophyll *a*

Net primary productivity (NPP) was calculated for each light incubation bottle by subtracting the initial DO concentration from the final DO concentration. To ensure that only metabolically active tissue (organic matter) was included in these analyses, values of NPP were corrected for ash-free dry weight (AFDW) using conversion factors established from standard regressions between blotted wet weight and AFDW (Freeman et al. 2013). Final values are thus expressed as mg O_2 l^{-1} g^{-1} AFDW. Photosymbiont abundance was estimated by measuring chl *a* concentrations of lyophilized sponge tissue from initial and treatment pieces of each species and was also corrected for AFDW using conversion factors from standard regressions between dry weight and AFDW (Freeman & Thacker 2011, Freeman et al. 2013).

Stable isotope analyses

Symbiont and host cell fractions were separated from bulk sponge tissue and prepared for isotope analyses, along with POM samples, using methods outlined for *Aplysina* spp. by Freeman & Thacker (2011) and Freeman et al. (2013). Stable isotope compositions were measured at the Carnegie Institution's Geophysical Laboratory using a Thermo Delta V Plus isotope ratio mass spectrometer coupled to a Carlo-Erba NC2500 elemental analyzer via a Conflo III open-split interface. Natural abundance isotope values (from initial samples and treatment replicates not used in the tracer experiment) are expressed in delta notation (δ) in units of per mil (‰) (see 3rd equation below, where 'sample' refers to either the microbial or sponge cell fraction from an individual and 'standard' refers to values of international standards of Vienna Pee Dee Belemnite and atmospheric N_2 for $\delta^{13}C$ and $\delta^{15}N$, respectively; Fry 2006). The formulas below are adapted for nitrogen by replacing ^{15}N and ^{14}N for ^{13}C and ^{12}C, respectively. The enrichment of samples used in the tracer experiment is expressed in atom percent excess (APE), which measures the increase in the atom percent of ^{13}C or ^{15}N in experimental samples compared to initial (or natural abundance) samples using formulas adapted from Fry (2006), Tanaka et al. (2006), and Weisz et al. (2010):

$$\text{APE } ^{13}C = \text{atom\% } ^{13}C \text{ in experimental sample} - \text{atom\% } ^{13}C \text{ in initial sample}$$

$$\text{atom\% } ^{13}C = [100 \times R_{standard} \times (\delta^{13}C \text{ sample} \div 1000 + 1)] \div [1 + R_{standard} \times (\delta^{13}C \text{ sample} \div 1000 + 1)]$$

$$\delta^{13}C = [(R_{sample} \div R_{standard}) - 1] \times 1000 \text{ with } R = {}^{13}C/{}^{12}C$$

Mean precision of $\delta^{13}C$ and $\delta^{15}N$ from 50 sets of duplicates from natural abundance samples was ±0.2 ‰ for both elements.

Unique interactions between *A. fulva* and *A. cauliformis* and their respective microbial communities might allow each of these species to utilize distinct sources of C and N at the same site (Freeman et al. 2014). To evaluate this hypothesis in the present study, we compared the niche area and relative position of symbiont and host fractions from initial individuals of *A. fulva* and *A. cauliformis* in bivariate isotopic ($\delta^{13}C$-$\delta^{15}N$) space using a Bayesian approach based on multivariate ellipse-based metrics (Stable Isotope Bayesian Ellipses in R [SIBER]), part of the SIAR package in R, as described by Jackson et al. (2011). We also compared ellipses between the 2 species within each treatment to highlight differential responses to experimental conditions. By generating Bayesian ellipses for each sample set, SIBER provides an unbiased, robust estimation of the relative niche area (standard ellipse area [SEA_c]) and position (% overlap between SEA_c of *A. fulva* and *A. cauliformis*) of a group within isotopic niche space (Jackson et al. 2011).

TGGE analyses

Whole genomic DNA was extracted from 78 samples using the Wizard Genomic DNA Purification Kit (Promega). Prior to PCR and TGGE analyses, optimal melting conditions and primer combinations required to resolve Clades A, B, and C of *Synechococcus spongiarum* were determined using WinMelt (Bio-Rad Laboratories). A small and highly variable

(~120 bp) fragment of the 16S-23S ITS region was amplified using the cyanobacterial-specific primers SynITS1F (5′-CTG TCA TCT CGA TGG TCG AT-3′) and modtIleR (5′-TCT AAC CAC CTG AGC TAA TGG C-3′). The reverse primer included a GC clamp (5′-CGC CCG CCG CGC GCT GAG CTA ATG GC-3′) attached to the 5′ end. Total PCR volume was 50 µl and was composed of 25 pmol of each primer, 10 nmol of each dNTP, 1× MasterTaq PCR Buffer (Eppendorf), 1× TaqMaster additive (Eppendorf), sterile water, 2 U of MasterTaq DNA polymerase (Eppendorf), and 1 µl of DNA template. PCR conditions consisted of an initial denaturing time of 5 min at 85°C, followed by 30 cycles of 1.5 min at 94°C, 2 min at 50°C, and 3 min at 72°C (Freeman 2012).

TGGE analyses were performed using a Bio-Rad DCode Universal Mutation Detection System (Bio-Rad, Germany) on a 6 M urea 8% (w/v) polyacrylamide gel in 1.25 Tris-acetate-EDTA buffer with a temperature gradient of 55 to 63°C and a ramp rate of 2°C. Electrophoresis was performed for 260 min (10 min at 55°C, 4 h run time, and 10 min at 63°C) at 110 V. All gels included experimental samples, negative controls, and samples of previously isolated standards for *S. spongiarum* Clades A, B, and C (Erwin & Thacker 2008b). Gels were stained for 30 min with GelRed (Biotium) and visualized and photographed using a Molecular Imager® Gel Doc System (Bio Rad). Bright DNA bands were excised using a sterile razor blade and stored in 50 µl of sterile distilled water overnight at 4°C, after which 1 µl of eluted PCR product was amplified using the above protocol with SynITS1F and modtIleR primers. PCR products from 2 replicate reactions per sample were pooled, gel purified, and sequenced on a Sanger sequencer at the University of Alabama at Birmingham (UAB) Center for AIDS Research (CFAR) DNA Sequencing Core Facility. Resulting sequences from forward and reverse reactions were aligned in CodonCode Aligner (CodonCode Corp.); GenBank BLAST searches identified the most closely related sequences. In all instances, bands from experimental samples that matched those of standards for *S. spongiarum* Clades A, B, and C run on the same gel were most closely related to published sequences from that clade. Changes in the *S. spongiarum* community across treatments were estimated qualitatively by the presence or absence of particular clades across samples using Image Lab 3.0 (Bio-Rad); values are expressed as the relative percentage of each clade recovered from individuals of each species from initial samples and each of the experimental treatments.

Data analysis

Since each canopy contained 2 replicates of each species, we initially compared differences in the mean values of growth rates and chl *a* concentrations using a general linear model (GLM; Systat, v. 11), testing the effects of treatment (control and S1 to S5), individual (1 to 10 of each species), and canopy within treatment (5 canopies per treatment). Because the effect of canopy within treatment was not significant in either species ($F = 1.08$, $p = 0.45$ and $F = 0.50$, $p = 0.85$ for growth rates of *A. cauliformis* and *A. fulva*, respectively, and $F = 1.95$, $p = 0.14$ and $F = 3.29$, $p = 0.18$ for chl *a* concentrations of *A. cauliformis* and *A. fulva*, respectively), future analyses tested only the effects of individual and treatment. Pairwise comparisons on treatment effects were carried out using the Fisher's least significant difference (LSD) post hoc test. For these and all subsequent analyses, residuals were tested for normality and homogeneity of variances among groups. Data not meeting assumptions of equal variance and normality were log- or rank-transformed prior to analyses.

Linear regressions determined whether trends in growth rate were related to photosymbiont abundance (absolute chl *a* concentration and relative change in chl *a* concentrations across treatments) or changes in the isotope values of sponge and microbial cell fractions ($\delta^{13}C$ or $\delta^{15}N$ of experimental samples – $\delta^{13}C$ or $\delta^{15}N$ of initial samples). Mean NPP values for each species were compared across control, S2, and S5 treatments using GLMs testing the effect of treatment blocked by individual. In addition, linear regressions were used to determine whether $APE^{13}C$ and $APE^{15}N$ values of both fractions were correlated with NPP values across treatments and to determine if $APE^{13}C$ and $APE^{15}N$ values of the sponge fraction were related to the $APE^{13}C$ and $APE^{15}N$ values of the corresponding microbial fraction. To assess differences in the presence of photosymbiont clades between species and among treatments, we used the function adonis in the R package vegan (Oksanen et al. 2014) to test the relative effects of species and treatment on the presence of specific clades within individual sponge samples.

RESULTS

Growth rates of *Aplysina cauliformis* varied significantly across treatments (general linear model [GLM]): $F = 5.58$, $p < 0.001$); highest growth rates were measured in individuals from treatments S1

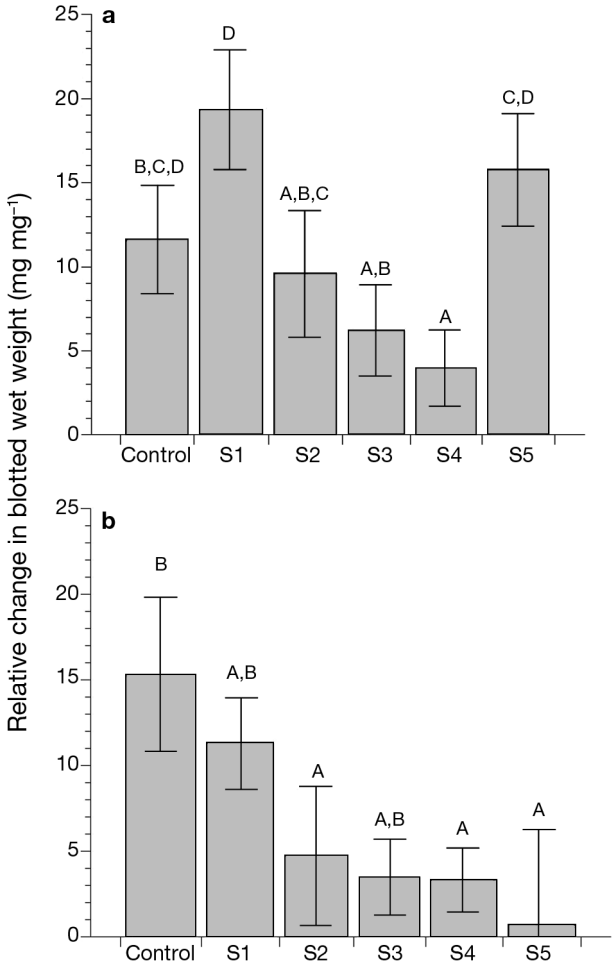

Fig. 1. Mean (±1 standard error) relative change in blotted wet weight in (a) *Aplysina cauliformis* and (b) *A. fulva* across 6 irradiance treatments (control and shade treatments S1 [1 layer of shade cloth] to S5 [5 layers of shade cloth]). Different letters above each treatment indicate statistically significant differences across treatments as determined by GLM followed by LSD multiple pairwise comparisons. In *A. cauliformis*: n = 7 (control), n = 8 (S1), n = 9 (S2), n = 10 (S3), n = 9 (S4), and n = 9 (S5). In *A. fulva*: n = 7 (control), n = 6 (S1), n = 6 (S2), n = 6 (S3), n = 8 (S4), and n = 7 (S5)

and S5, while growth under intermediate irradiances in treatments S3 and, especially, S4 was significantly reduced (Fig. 1a). In *A. fulva*, by contrast, growth rate was low across shade treatments (GLM: $F = 2.45$, p = 0.06, Fig. 1b). Surprisingly, photosymbiont abundance, as measured by chl *a* values, followed similar trends in both species but varied little across treatments (GLM on log-transformed data: $F = 1.20$, p = 0.33 and $F = 0.92$, p = 0.49 for *A. cauliformis* and *A. fulva*, respectively; Fig. S1 in the supplement at www.int-res.com/articles/suppl/m526p041_supp.pdf). In addition, neither absolute chl *a* concentration nor relative change in chl *a* was strongly correlated with growth rate in *A. cauliformis* (linear regression: $r^2 = 0.01$, $F = 0.67$, p = 0.42 and $r^2 < 0.01$, $F = 0.03$, p = 0.85 for absolute chl *a* concentration and relative change in chl *a*, respectively) or in *A. fulva* (linear regression: $r^2 < 0.01$, $F = 0.27$, p = 0.61 and $r^2 < 0.01$, $F = 0.21$, p = 0.65 for absolute chl *a* concentration and relative change in chl *a*, respectively).

There was substantial variation in the stable isotope ratios ($\delta^{13}C$ and $\delta^{15}N$) of the microbial and sponge cell fractions of both species across treatments (Fig. S2). In *A. cauliformis*, 36% ($r^2 = 0.36$, $F = 18.33$, $p < 0.001$) and 63% ($r^2 = 0.63$, $F = 55.82$, $p < 0.0001$) of the variation in the $\delta^{13}C$ and $\delta^{15}N$ values of the sponge fraction were explained by the $\delta^{13}C$ and $\delta^{15}N$ values of the corresponding microbial fraction (Fig. S3). In contrast, in *A. fulva*, 11% ($r^2 = 0.11$, $F = 3.10$, p = 0.09) and 29% ($r^2 = 0.29$, $F = 10.52$, $p < 0.01$) of the variation in the sponge $\delta^{13}C$ and $\delta^{15}N$ values were explained by the $\delta^{13}C$ and $\delta^{15}N$ values of the corresponding microbial fraction (Fig. S4).

Enrichment in $\delta^{13}C$ values of the microbial ($r^2 = 0.21$, $F = 9.0$, $p < 0.01$; Fig. 2a) and sponge ($r^2 = 0.36$, $F = 18.87$, $p < 0.001$) cell fractions across treatments was inversely correlated with growth rate in *A. cauliformis*, but shifts in $\delta^{13}C$ values were not correlated with growth rate in *A. fulva* (microbial fraction: $r^2 = 0.04$, $F = 1.07$, p = 0.31; Fig. 2b; and sponge fraction: $r^2 = 0.002$, $F = 0.04$, p = 0.84). Likewise, shifts in $\delta^{15}N$ values across treatments were inversely correlated with growth rates in *A. cauliformis* ($r^2 = 0.14$, $F = 5.59$, p = 0.02 and $r^2 = 0.14$, $F = 5.39$, p = 0.03 for sponge and microbial fractions, respectively; Fig. S5a) but not in *A. fulva* ($r^2 = 0.02$, $F = 0.50$, p = 0.49 and $r^2 < 0.01$, $F = 0.05$, p = 0.82 for sponge and microbial fractions, respectively; Fig. S5b).

Holobiont net primary productivity (NPP) was strongly impacted by shading treatments. Although NPP was more variable across treatments in *A. fulva* (GLM: $F = 9.87$, p = 0.047) than in *A. cauliformis* (GLM: $F = 5.11$, p = 0.062), NPP values of both species from shading treatment S5 were significantly reduced compared to individuals from control canopies, and individuals of both *A. cauliformis* and *A. fulva* from treatment S2 had intermediate NPP values (Fig. 3). In both species, variation in NPP across treatments was correlated with the ^{13}C enrichment of the microbial fraction ($r^2 = 0.43$, $F = 7.5$, p = 0.02 for *A. cauliformis* and $r^2 = 0.43$, $F = 6.0$, p = 0.04 for *A. fulva*; Fig. 4). However, NPP and ^{13}C enrichment of the sponge fraction were only correlated in *A. cauliformis* ($r^2 = 0.38$, $F = 6.01$,

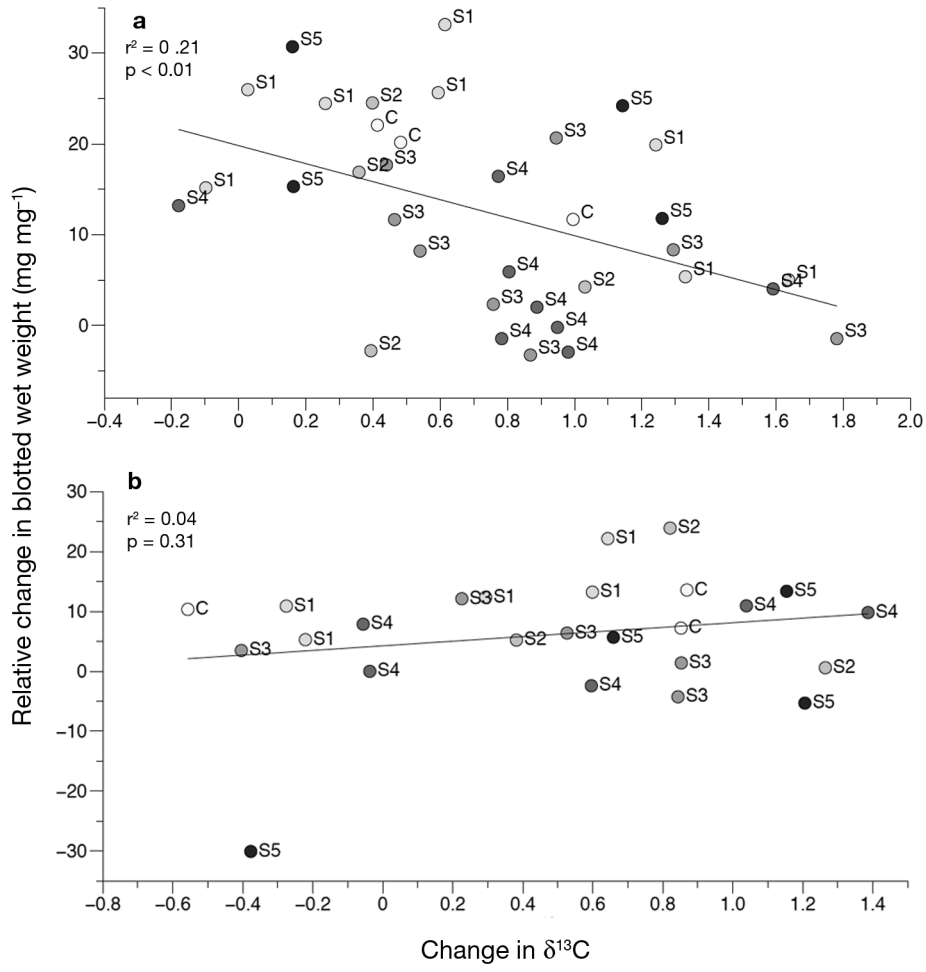

Fig. 2. Sponge growth rate (relative change in blotted wet weight) as a function of change in the $\delta^{13}C$ values of the microbial fraction in (a) *Aplysina cauliformis* and (b) *A. fulva* across 6 irradiance treatments (control [C] and shade treatments S1 [1 layer of shade cloth] to S5 [5 layers of shade cloth])

p = 0.03 for *A. cauliformis* and $r^2 < 0.01$, $F = 0.01$, p = 0.92 for *A. fulva*; Fig. 4). Although NPP and the ^{15}N enrichment of microbial cells were also correlated in both species ($r^2 = 0.62$, $F = 16.07$, $p < 0.01$ and $r^2 = 0.60$, $F = 11.95$, $p < 0.01$ for *A. cauliformis* and *A. fulva*, respectively; Fig. S6), NPP was not correlated with the ^{15}N enrichment of the sponge fraction in either species ($r^2 = 0.28$, $F = 3.88$, p = 0.08 and $r^2 = 0.37$, $F = 4.73$, p = 0.06 for *A. cauliformis* and *A. fulva*, respectively; Fig. S6).

Microbial and sponge metabolism were strongly coupled in *A. cauliformis*, with approximately 88% of the variability in ^{13}C enrichment and 48% of the variability in ^{15}N enrichment of the sponge fraction attributable to ^{13}C or ^{15}N enrichment in the corresponding microbial fraction ($r^2 = 0.88$, $F = 71.24$, $p < 0.001$ and $r^2 = 0.48$, $F = 9.4$, p = 0.01 for ^{13}C and ^{15}N enrichment, respectively; Fig. S7). In contrast, in *A. fulva*, only 13% of the variability in sponge ^{13}C enrichment was attributable to ^{13}C enrichment of the corresponding microbial fraction ($r^2 = 0.13$, $F = 1.21$, p = 0.30; Fig. S8a). Over 50% of the variability in ^{15}N enrichment of the sponge fraction of *A. fulva* could be explained by ^{15}N enrichment in the corresponding microbial fraction ($r^2 = 0.52$, $F = 8.5$, p = 0.02; (Fig. S8b).

Although the sizes of the standard ellipse areas (niche area; SEA_C) of both fractions were similar in initial individuals of both *A. fulva* and *A. cauliformis* (SIBER analysis: $p > 0.05$), there was only a 12% overlap of the ellipses representing the sponge fractions of these species (Fig. 5). In comparison, ellipses of the microbial fractions overlapped by almost 50% (Fig. 5). Niche areas of these species were also similar in all experimental treatments (SIBER analysis: $p > 0.05$); the percentage of overlap of the sponge

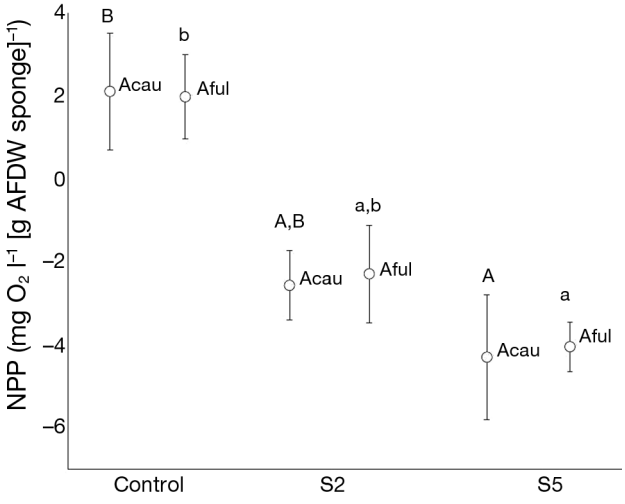

Fig. 3. Mean (±1 SE) net primary productivity (NPP) in individuals of *Aplysina cauliformis* (Acau) and *A. fulva* (Aful) from control, intermediate (S2), and full shade (S5) treatments. Different letters indicate statistically significant differences across treatments within each species (uppercase letters for *A. cauliformis* and lowercase letters for *A. fulva*) determined by GLM followed by LSD multiple pairwise comparisons. n = 4 for control of both species and treatments S2 and S5 of *A. cauliformis*; n = 3 for treatments S2 and S5 of *A. fulva*

fraction ellipses was on average ~30% less than that of the microbial fraction.

Clade A of *Synechococcus spongiarum* was present in all of the 78 samples analyzed using TGGE, regardless of species, while Clade B was present in 81% of all samples (82% of *A. cauliformis* samples and 80% of *A. fulva* samples). Clade C was found in 22% of all samples analyzed (13% of *A. cauliformis* samples and 30% of *A. fulva* samples), while the less abundant Clades D and K were only observed in 12% (13% of *A. cauliformis* samples and 10% of *A. fulva* samples) and 18% (21% of *A. cauliformis* samples and 15% of *A. fulva* samples) of samples, respectively. Species accounted for only ~1% of the variation in cladal structure across individuals (adonis effect of species: $r^2 = 0.01$, $F = 1.12$, $p = 0.3$). In addition, although there was evidence for the loss of single clades in some individual samples (Clade D of both species and Clade C of *A. cauliformis*) under different shading treatments, these trends were only observed in single individuals, and there was minimal variation in the presence or absence of clades across treatments (adonis effect of treatment: $r^2 = 0.01$, $F = 0.18$, $p = 0.9$; Fig. 6).

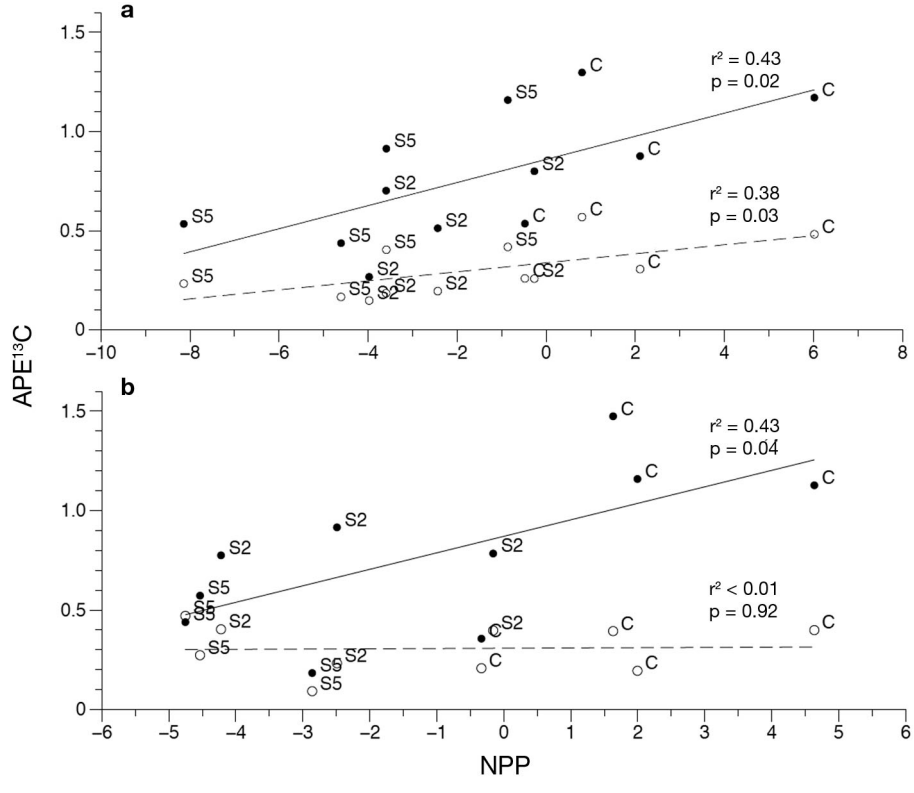

Fig. 4. APE^{13}C of microbial (solid line) and sponge (dashed line) fractions of (a) *Aplysina cauliformis* and (b) *A. fulva* as a function of net primary productivity (NPP) in individuals from control (C), intermediate shade (S2), and full shade (S5) treatments

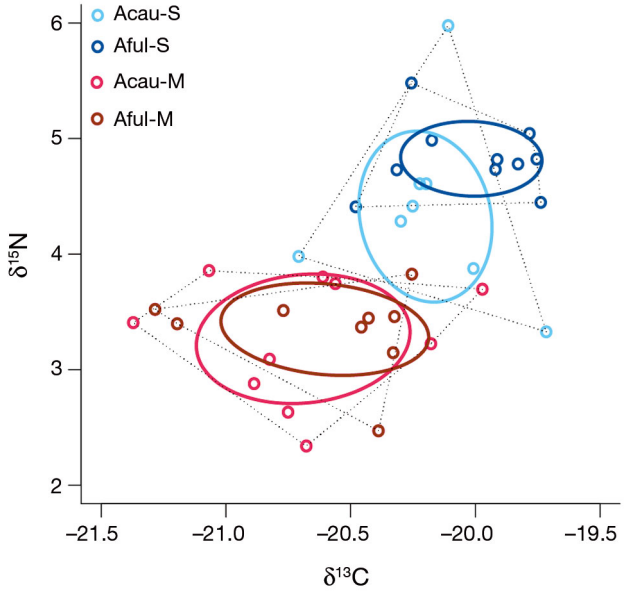

Fig. 5. $\delta^{13}C$ and $\delta^{15}N$ bi-plot of microbial (M) and sponge (S) fractions from initial samples of *Aplysina cauliformis* (Acau) and *A. fulva* (Aful). Solid lines depicting the isotopic niche space of each fraction of both species were calculated as standard ellipse areas (SEA_C). Convex hulls depicting total niche width are also shown with dashed lines for reference. n = 10 for sponge fractions of both species and the microbial fraction of *A. cauliformis*; n = 9 for the microbial fraction of *A. fulva*

DISCUSSION

Our results support the hypotheses that (1) 2 closely related host species, *Aplysina cauliformis* and *A. fulva*, have unique interactions with their symbiotic microbial communities and (2) that these interactions influence holobiont responses to environmental change (Freeman & Thacker 2011). In *A. fulva*, as expected from previous shading experiments, the net benefit of the interaction to the host was low under shade treatments (Fig. 1, Freeman & Thacker 2011). In contrast, although the growth of *A. cauliformis* was similar under control and full shade treatments (Freeman & Thacker 2011), we measured a surprising reduction in net benefit to the host under intermediate irradiances (Fig. 1).

Shifts in the net benefit of a symbiosis under changing environmental conditions are commonly ascribed to altered abundances of symbionts, with changes in host growth rates under experimental shading frequently linked to a reduction in photosymbiont abundance (Thacker 2005, Erwin & Thacker 2008a, Freeman & Thacker 2011, Thacker & Freeman 2012). Counter to this hypothesis, in the present study, there were no significant differences in chl *a* concentrations across treatments (Fig. S1), and individual growth rates were not correlated with either absolute chl *a* concentrations or relative changes in chl *a* concentrations. These findings support the hypothesis that, in sponge-microbe interactions, symbiont metabolism, but not necessarily overall symbiont abundance, is a driving force in host performance (Freeman et al. 2013, 2014).

To assess whether trends in growth rate were driven by shifts in the assimilation of symbiont-derived C and N, we analyzed the stable isotope ratios of carbon and nitrogen ($\delta^{13}C$ and $\delta^{15}N$) in isolated sponge cell fractions and compared these values to those from microbial cell fractions isolated from the same individual and POM filtered from the water column (Freeman & Thacker 2011). Sponge $\delta^{13}C$ values of both species were >4‰ more enriched than POM but were approximately 1‰ more en-

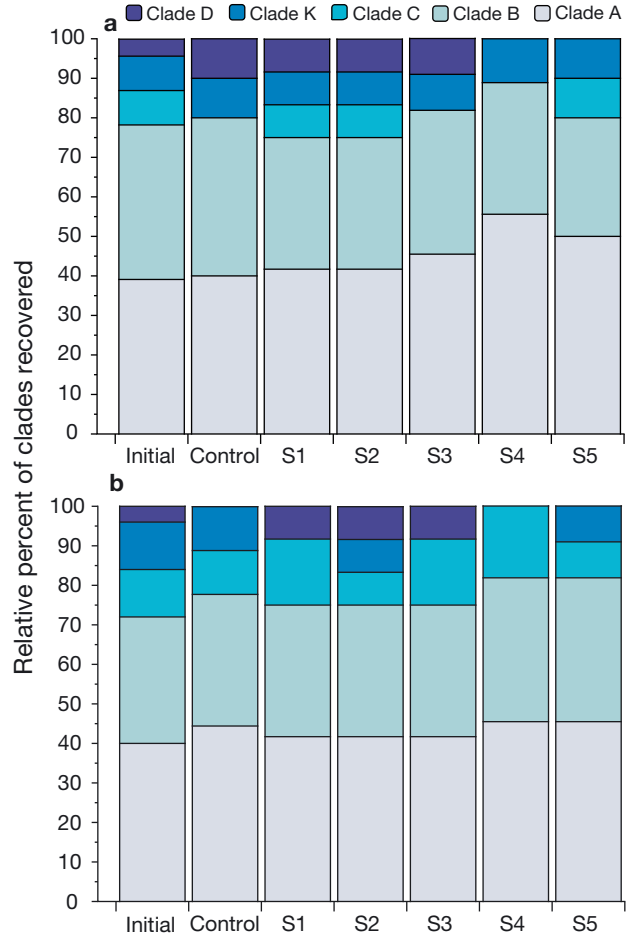

Fig. 6. Relative percentage of *Synechococcus spongiarum* clades A, B, C, D, and K recovered from initial and experimental (control and shade treatments S1 [1 layer of shade cloth] to S5 [5 layers of shade cloth]) samples of (a) *Aplysina cauliformis* and (b) *A. fulva*

riched than their corresponding microbial fraction. Likewise, sponge cell $\delta^{15}N$ values were enriched by approximately 1‰ compared to their corresponding microbial fraction and were at or slightly above the mean $\delta^{15}N$ value of POM (Fig. S2). Using published fractionation values (Fry 2006, Freeman & Thacker 2011), it thus appears as though both of these species are assimilating C and N from their microbial communities. Importantly, because the sponge fractions of both species do not become significantly depleted in $\delta^{13}C$ and enriched in $\delta^{15}N$ under shade treatments, it is likely that neither of these species increase their assimilation of heterotrophically derived C and N from POM under reduced irradiances.

There was, however, substantial enrichment in the $\delta^{13}C$ and $\delta^{15}N$ values of the microbial fractions of both species across the shade treatments (up to ~1.8‰ and 1.2‰ for the $\delta^{13}C$ and $\delta^{15}N$ values of *A. cauliformis* and ~1.4‰ and 1.1‰ for the $\delta^{13}C$ and $\delta^{15}N$ values of *A. fulva*). Enrichment in symbiont $\delta^{13}C$ and $\delta^{15}N$ values might reflect reduced isotopic discrimination during C and N assimilation, increased assimilation of a ^{13}C- or ^{15}N-enriched C or N source, or changes in the C and N cycling within the holobiont under some irradiance treatments (Muscatine et al. 1989, Muscatine & Kaplan 1994, Swart et al. 2005). Although our understanding of factors driving enrichment in symbiont $\delta^{13}C$ and $\delta^{15}N$ values in the present study is limited, each of these species responded differently to these shifts in isotopic composition. In *A. cauliformis*, symbiont and host C and N metabolism were tightly coupled (Figs. S3 & S7), and these shifts were correlated with a reduction in the net benefit (host growth rate) of the symbiosis (Fig. 2a, Fig. S5a; Freeman & Thacker 2011). In contrast, symbiont and host C metabolism were weakly coupled in *A. fulva*, and host growth rate was not correlated with changes in symbiont C and N metabolism (Fig. 2b, Figs. S4, S5b, & S8). Thus, the comparatively low assimilation of symbiont-derived C by *A. fulva* under ambient irradiances (Freeman & Thacker 2011) might be further reduced by the decoupling of host and symbiont metabolism under lower irradiances.

Correlations between NPP and the $APE^{13}C$ and $APE^{15}N$ of the microbial fractions of both species suggest that photosymbiont metabolism is an important driver of shifts in holobiont C and N metabolism (Fig. 4, Fig. S6). In *A. cauliformis*, NPP and $APE^{13}C$ values of the sponge fraction were also correlated (Fig. 4a), supporting the contention that photosymbiont-derived C benefit is directly related to holobiont productivity (Freeman et al. 2013). In *A. fulva*, on the other hand, $APE^{13}C$ values of the sponge fraction were low regardless of holobiont productivity (Fig. 4b), supporting the assertion that host and photosymbiont metabolism are weakly coupled in this species (Freeman & Thacker 2011). Carbon metabolism in this species might be supplemented by local sources such as portions of the POM pool or dissolved organic matter (DOM) that would not be reflected in ^{13}C enrichments (Fig. 5; van Duyl et al. 2011, de Goeij et al. 2013). Likewise, $APE^{15}N$ values of the sponge fractions of both species were not correlated with NPP (Fig. S6), supporting the assertion that a symbiont-derived N benefit to these hosts (Figs. S3b, S4b, & S6) is likely driven by a combination of photosymbionts and other microbial taxa capable of diverse N transformations (Fiore et al. 2010, Freeman et al. 2013) or local allochthonous sources of N.

It is important to note that both of these species could be feeding on DOM or selectively feeding on a specific portion of the POM pool (picoplankton or nanoeukaryotic cells), both of which might be underrepresented by bulk POM $\delta^{13}C$ and $\delta^{15}N$ values (van Duyl et al. 2011, Maldonado et al. 2012, de Goeij et al. 2013). Without a more detailed understanding of $\delta^{13}C$ and $\delta^{15}N$ variation across different size classes, taxa, or types of food sources, it is difficult to firmly establish the trophic interactions of diverse sponge species. In addition, although some of our conclusions have been adapted from published fractionation values (Michener & Schell 1994, Freeman 2001) that are well established across other taxa, we still need quantitative measurements of how sponge hosts fractionate diverse sources of C and N.

Because trends in holobiont productivity and C metabolism could be driven by the presence or absence of particular clades of the sponge-specific cyanobacterial symbiont *Synechococcus spongiarum* (Freeman et al. 2013), we used TGGE to assess whether shifts in photosymbiont communities occurred under different shade treatments. In an extensive survey of clades of *S. spongiarum*, Erwin & Thacker (2008b) found 13 distinct clades of this symbiont within 18 species of sponges throughout the Caribbean. In Bocas del Toro, *A. cauliformis* was previously reported to only host Clade B, whereas only Clades A and B were previously reported within *A. fulva* collected from this site (Erwin & Thacker 2008b). Thus, the present study represents the first report of Clades C, D, and K within both of these *Aplysina* species as well as the first report of Clade A in *A. cauliformis* from Bocas del Toro. Surprisingly, both species hosted similar communities of *S. spongiarum*, and the presence of these clades remained

stable regardless of treatment (Fig. 6). Thus, this study does not support the hypothesis that genetic diversity of *S. spongiarum* is driving growth trends or stable isotope ratios across treatments and provides no evidence to support the hypothesis that these photosymbiont communities are shifting across different irradiance treatments. Additional studies utilizing next-generation sequencing technology targeting the 16S-23S ITS region may further elucidate the genetic diversity of *S. spongiarum* in diverse sponge hosts and may allow us to better quantify shifts in these communities under changing environmental conditions. In addition, it is likely that shifts in the abundance of other members of these microbial communities are occurring. Future work coupling manipulative experiments like these with 16S rRNA metagenomics using next-generation sequencing may also help to elucidate whether changes in sponge growth rates and holobiont C and N metabolism are driven by shifts in microbial community composition (Thacker & Freeman 2012).

Fundamental differences in the interactions of 2 closely related sponge species and their microbial symbiont communities raise important questions about the evolution and maintenance of these symbioses. For instance, although it appears that host performance is strongly and weakly coupled to symbiont metabolism in *A. cauliformis* and *A. fulva*, we can only hypothesize as to what forces might drive this variation across species. *A. cauliformis* might actively engage in the reciprocal exchange of resources with its symbiont community or may enhance symbiont metabolism under certain conditions via the release of host factors (Gates et al. 1995). Active control of its symbiont community might help explain how *A. cauliformis* is able to maintain high growth rates, even under reduced irradiance. *A. fulva*, in contrast, hosts symbionts but might only passively obtain the products of symbiont metabolism when available. These 2 species might also be on different evolutionary trajectories, with their divergence driven by multiple factors both intrinsic and extrinsic to the interaction (Herre et al. 1999, Stat et al. 2008, Kiers et al. 2010, Thacker & Freeman 2012). For instance, the decoupling of symbiont and host C metabolism in *A. fulva* might be reflective of a shift in which previously beneficial photosymbionts begin to cheat by withholding excess C from *A. fulva*. Such cheating is widespread in many mutualisms and may result in the slow erosion of this mutualism (Bronstein et al. 2004). Alternatively, disparity in the overlap of the ellipses representing the sponge fractions of each species, despite an overlap of approximately 50% for the ellipses of the microbial fractions, suggests that these 2 hosts might each be utilizing unique sources of C and N at this site. While a larger sample size is needed to explicitly test this hypothesis, such divergence might allow for the exploitation of novel niche spaces on these shallow reefs (Freeman et al. 2014) or might reflect a diminished role of symbiosis in some species as eutrophic conditions become more prevalent in many coastal communities (Baker et al. in press). Identifying whether such divergence is restricted to this local population or if similar trends are observed throughout the Caribbean and in other sympatric host species is an important next step.

Finally, this study supports the hypothesis that there is a dynamic relationship between the net benefit of a symbiotic interaction and environmental conditions (Boucher et al. 1982, Thacker & Freeman 2012, Johnson & Graham 2013). Although this net benefit is driven by the complex interplay of benefits and costs, our results are largely explained in terms of changes in symbiont provisioning (benefit) alone because the potential costs to a sponge host are largely speculative and difficult to quantify (Thacker & Freeman 2012). Despite this, because physiological and ecological costs might set limits on where certain host species can exist and under what conditions beneficial interactions become antagonistic (Bronstein 2001), a better understanding of these costs, and how they change with environmental conditions, is critical if we are to predict how particular species or functional groups will respond to environmental change.

Acknowledgements. We thank R. Collin, G. Jacome, and P. Gondola at the Smithsonian Tropical Research Institute Bocas Research Station and M. Fogel and R. Bowden at the Geophysical Laboratory for their technical assistance and logistical support. K. Erickson provided field assistance. Financial support for this project came from a Smithsonian Tropical Research Short-Term Fellowship, a Sigma Xi Grants-in-Aid of Research to C.J.F., US National Science Foundation Grants 0726944 and 0829986 to R.W.T. and a Smithsonian Institution Marine Science Network Postdoctoral Fellowship awarded to D.M.B.

LITERATURE CITED

Baker DM, Freeman CJ, Knowlton N, Thacker RW, Kim K, Fogel ML (in press) Productivity links morphology, symbiont specificity, and bleaching in the evolution of Caribbean octocoral symbioses. ISME J

Barneah O, Weis VM, Perez S, Benayahu Y (2004) Diversity of dinoflagellate symbionts in Red Sea soft corals: mode of symbiont acquisition matters. Mar Ecol Prog Ser 275: 89–95

Boucher DH, James S, Keeler KH (1982) The ecology of mutualism. Annu Rev Ecol Syst 13:315–347

Bronstein JL (2001) The costs of mutualism. Am Zool 41: 825–839

Bronstein JL, Dieckmann U, Ferrière R (2004) Coevolutionary dynamics and the conservation of mutualisms. In: Ferrière R, Dieckmann U, Couvet D (eds) Evolutionary conservation biology. Cambridge University Press, Cambridge, p 305–326

Cowden CC, Peterson CJ (2009) A multi-mutualist simulation: applying biological market models to diverse mycorrhizal communities. Ecol Model 220:1522–1533

Dattagupta S, Schaperdoth I, Montanari A, Mariani S, Kita N, Valley JW, Macalady JL (2009) A novel symbiosis between chemoautotrophic bacteria and a freshwater cave amphipod. ISME J 3:935–943

de Goeij JM, van Oevelen D, Vermeij MJA, Osinga R, Middelburg JJ, de Goeij AFPM, Admiraal W (2013) Surviving in a marine desert: the sponge loop retains resources within coral reefs. Science 342:108–110

Easson CG, Thacker RW (2014) Phylogenetic signal in the community structure of host-specific microbiomes of tropical marine sponges. Front Microbiol 5:532

Erwin PM, Thacker RW (2007) Incidence and identity of photosynthetic symbionts in Caribbean coral reef sponge assemblages. J Mar Biol Assoc UK 87:1683–1692

Erwin PM, Thacker RW (2008a) Phototrophic nutrition and symbiont diversity of two Caribbean sponge–cyanobacteria symbioses. Mar Ecol Prog Ser 362:139–147

Erwin PM, Thacker RW (2008b) Cryptic diversity of the symbiotic cyanobacterium *Synechococcus spongiarum* among sponge hosts. Mol Ecol 17:2937–2947

Fiore CL, Jarett JK, Olson ND, Lesser MP (2010) Nitrogen fixation and nitrogen transformations in marine symbioses. Trends Microbiol 18:455–463

Freeman KH (2001) Isotopic biogeochemistry of marine organic carbon. In: Valley JW, Cole DR (eds) Stable isotope geochemistry. The Mineralogical Society of America, Washington, DC, p 579–597

Freeman CJ (2012) Complex interactions between marine sponges and their symbiotic microbial communities. PhD dissertation, University of Alabama at Birmingham, Birmingham, AL

Freeman CJ, Thacker RW (2011) Complex interactions between marine sponges and their symbiotic microbial communities. Limnol Oceanogr 56:1577–1586

Freeman CJ, Thacker RW, Baker DM, Fogel M (2013) Quality or quantity: Is nutrient transfer driven more by symbiont identity and productivity than by symbiont abundance? ISME J 7:1116–1125

Freeman CJ, Easson CG, Baker DM (2014) Metabolic diversity and niche structure in sponges from the Miskito Cays, Honduras. Peer J 2:e695

Fry B (2006) Stable isotope ecology. Springer, New York, NY

Gates RD, Hoegh-Guldberg O, McFall-Ngai MJ, Bil KY, Muscatine L (1995) Free amino acids exhibit anthozoan 'host factor' activity: they induce the release of photosynthate from symbiotic dinoflagellates *in vitro.* Proc Natl Acad Sci USA 92:7430–7434

Herre EA, Knowlton N, Mueller UG, Rehner SA (1999) The evolution of mutualisms: exploring the paths between conflict and cooperation. Trends Ecol Evol 14:49–53

Jackson AL, Inger R, Parnell A, Bearhop S (2011) Comparing isotopic niche widths among and within communities: SIBER-Stable Isotope Bayesian Ellipses in R. J Anim Ecol 80:595–602

Johnson NC, Graham JH (2013) The continuum concept remains a useful framework for studying mycorrhizal functioning. Plant Soil 363:411–419

Kiers ET, Palmer TM, Ives AR, Bruno JF, Bronstein JL (2010) Mutualisms in a changing world: an evolutionary perspective. Ecol Lett 13:1459–1474

Maldonado M, Ribes M, van Duyl FC (2012) Nutrient fluxes through sponges: biology, budgets, and ecological implications. Adv Mar Biol 62:113–182

Michener RH, Schell DM (1994) Stable isotope ratios as tracers in marine aquatic food webs. In: Lajtha K, Michener RH (eds) Stable isotopes in ecology and environmental science. Blackwell Scientific Publications, Oxford, p 138–157

Muscatine L, Kaplan IR (1994) Resource partitioning by reef corals as determined from stable isotope composition II. $\delta^{15}N$ of zooxanthellae and animal tissue versus depth. Pac Sci 48:304–312

Muscatine L, Porter JW, Kaplan IR (1989) Resource partitioning by reef corals as determined from stable isotope composition I. $\delta^{13}C$ of zooxanthellae and animal tissue vs depth. Mar Biol 100:185–193

Nyholm SV, McFall-Ngai MJ (2004) The winnowing: establishing the squid-*Vibrio* symbiosis. Nat Rev Microbiol 2: 632–642

Oksanen J, Blanchet FG, Kindt R, Legendre P and others (2014) Vegan: community ecology package. Available at: http://cran.r-project.org/web/packages/vegan

Schmitt S, Tsai P, Bell J, Fromont J and others (2012) Assessing the complex sponge microbiota: core, variable, and species-specific bacterial communities in marine sponges. ISME J 6:564–576

Stanley GD Jr (2006) Photosymbiosis and the evolution of modern coral reefs. Science 312:857–858

Stat M, Morris E, Gates RD (2008) Functional diversity in coral-dinoflagellate symbiosis. Proc Natl Acad Sci USA 105:9256–9261

Steinert M, Hentschel U, Hacker J (2000) Symbiosis and pathogenesis: evolution of the microbe-host interaction. Naturwissenschaften 87:1–11

Swart PK, Saied A, Lamb K (2005) Temporal and spatial variation in the $\delta^{15}N$ and $\delta^{13}C$ of coral tissue and zooxanthellae in *Montastrea faveolata* collected from the Florida reef tract. Limnol Oceanogr 50:1049–1058

Tanaka Y, Miyajima T, Koike I, Hayashibara T, Ogawa H (2006) Translocation and conservation of organic nitrogen within the coral-zooxanthellae symbiotic system of *Acropora pulchra*, as demonstrated by dual isotope-labeling techniques. J Exp Mar Biol Ecol 336:110–119

Taylor MW, Radax R, Steger D, Wagner M (2007) Sponge-associated microorganisms: evolution, ecology, and biotechnological potential. Microbiol Mol Biol Rev 71: 295–347

Thacker RW (2005) Impacts of shading on sponge-cyanobacteria symbioses: a comparison between host-specific and generalist associations. Integr Comp Biol 45: 369–376

Thacker RW, Freeman CJ (2012) Sponge-microbe symbioses: recent advances and new directions. Adv Mar Biol 62:57–111

van Duyl FC, Moodley L, Nieuwland G, van Ijzerloo L and others (2011) Coral cavity sponges depend on reef-derived food resources: stable isotope and fatty acid constraints. Mar Biol 158:1653–1666

Venn AA, Loram JE, Douglas AE (2008) Photosynthetic symbioses in animals. J Exp Bot 59:1069–1080

Vrijenhoek RC (2010) Genetics and evolution of deep-sea chemosynthetic bacteria and their invertebrate hosts. In: Kiel S (ed) The vent and seep biota, Topics in Geobiology 33. Springer, Berlin, p 15–50

Webster NS, Taylor MW, Behnam F, Lücker S and others (2010) Deep sequencing reveals exceptional diversity and modes of transmission for bacterial sponge symbionts. Environ Microbiol 12:2070–2082

Weisz JB, Hentschel U, Lindquist N, Martens CS (2007) Linking abundance and diversity of sponge-associated microbial communities to metabolic differences in host sponges. Mar Biol 152:475–483

Weisz JB, Massaro AJ, Ramsby BD, Hill MS (2010) Zooxanthellar symbionts shape host sponge trophic status through translocation of carbon. Biol Bull 219:189–197

Wilkinson CR (1983) Net primary productivity in coral reef sponges. Science 219:410–412

Wooldridge SA (2010) Is the coral-algae symbiosis really 'mutually beneficial' for the partners? BioEssays 32: 615–625

Wooldridge SA (2013) Breakdown of the coral-algae symbiosis: towards formalising a linkage between warm-water bleaching thresholds and the growth rate of the intracellular zooxanthellae. Biogeosciences 10:1647–1658

Zilber-Rosenberg I, Rosenberg E (2008) Role of microorganisms in the evolution of animals and plants: the hologenome theory of evolution. FEMS Microbiol Rev 32:723–735

Editorial responsibility: Joseph Pawlik, Wilmington, NC, USA

Submitted: September 24, 2014; Accepted: February 20, 2015
Proofs received from author(s): April 6, 2015